Chapter 3

Interpolation of missing offset traces

3.1 Introduction

The wavefront synthesis algorithm explained in the previous chapter implicitly assumes that a data set is collected with source and receiver spacings short enough to avoid spatial aliasing and with a large receiver cable long enough to avoid artifacts caused by a truncated aperture. In practice, however, the data are usually collected with a finite source spacing and a finite receiver length, as well as some missing near offset traces. The former can introduce spatial aliasing, while the latter causes the problems of end-effects.

If we are only interested in structural imaging, weak or broken images are not a significant problem. Such image artifacts will disappear after the stacking of several images generated by different plane-wave synthesis. If we are interested in angle-dependent reflectivity, however, each image from a different plane-wave needs to be analyzed separately. Therefore, the missing traces should be interpolated to produce a complete image without artifacts in it.

Fowler (1985) proposes a method that finds zero-offset traces by fitting a polynomial to the amplitudes as a function of offset after NMO correction. However, this method requires accurate stacking velocity before interpolation. In this chapter, I introduce an interpolation scheme for missing traces in near and far offset, which does not require velocity estimation for each events. First I review the forward model of a shot experiment and wave stack that allows the wavefront synthesis. I then present the detailed algorithm of the interpolation scheme, along with some examples of synthetic and Marmousi data sets.

3.2 End-effects caused by a finite aperture

The ideal acquisition pattern for plane-wave synthesis is a fixed-split spread with wide aperture (Figure 3.1). With this acquisition, every receiver will record reflected wave fields caused by every source wave field. In practice, however, a moving one-side spread (Figure 3.2) is the typical acquisition pattern in marine surveys.

The forward model in equation (2.1) implicitly assumes an infinite aperture experiment. In order to model correctly, we need to incorporate the aperture effect as follows:

$$\mathbf{g}_j(z_0) = A_j F(z_0, z_0)\mathbf{s}_j(z_0), \tag{3.1}$$

where A_j is a diagonal matrix with 1, where the receiver is located and 0 elsewhere. Since the aperture operator, A_j, changes from source to source in a moving one-side spread, the wave-stack equation (2.3) is no longer valid. In order to overcome this problem, we need to fill the missing traces before wave stacking.

In the case of the one-sided spread acquisition, we can expand the acquisition area using the principle of reciprocity, which states that if we exchange the source and receiver positions, we would record the same seismic trace at the source position. The acquisition pattern is expanded using the principle of reciprocity as depicted in Figure 3.3.

However, Figure 3.3 shows that we still have some missing regions in near and far offset after the acquisition expansion that uses the principle of reciprocity. The missing part of the far-offset limits the angle coverage of the reflectivity information. Since the maximum incidence angle of the source wave field generally decreases as the depth of reflector increases (Figure 3.4), we can avoid the effects of cable length by synthesizing different incidence angle ranges at every depth level.

The effects of the missing part of the near offset are not as easily avoided as those of the missing part of the far offset, because the effect of missing near-offset traces differ in terms of missing reflection angle ranges from depth to depth and are located around the normal incidence angle to reflectors (Figure 3.4). In order to obtain a good image in every constant angle illumination, we need to interpolate the missing near offset traces.

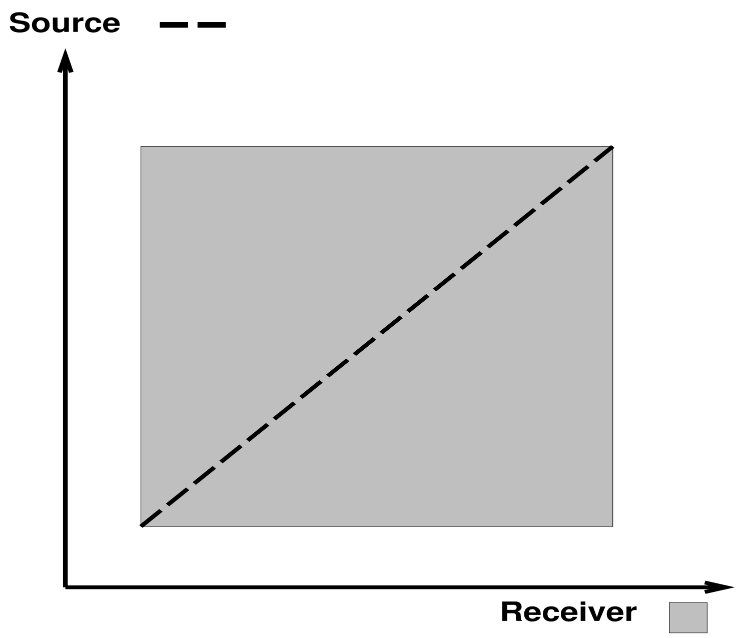

FIG. 3.1. A fixed split-spread acquisition that is ideal for wavefront synthesis imaging. (interp-ideal-acq) [NR]

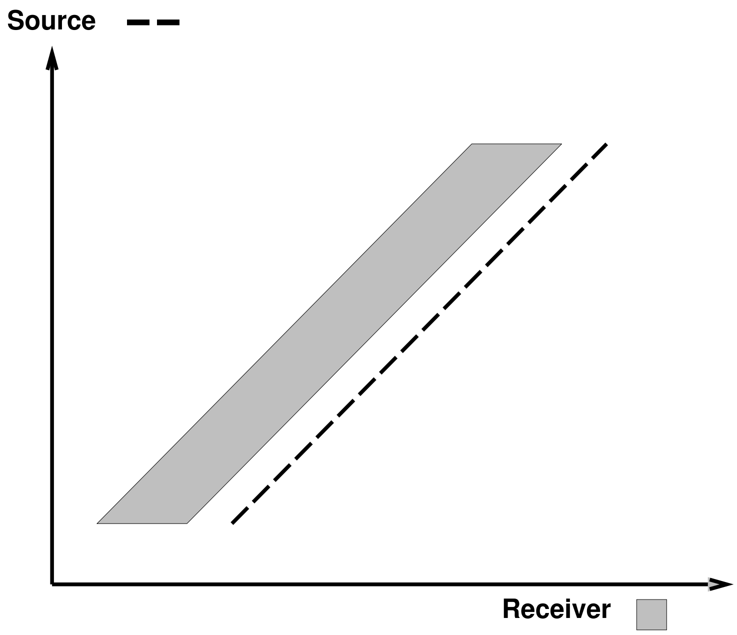

FIG. 3.2. A one-side spread acquisition, which is the typical acquisition pattern in a marine survey. (interp-real-acq) [NR]

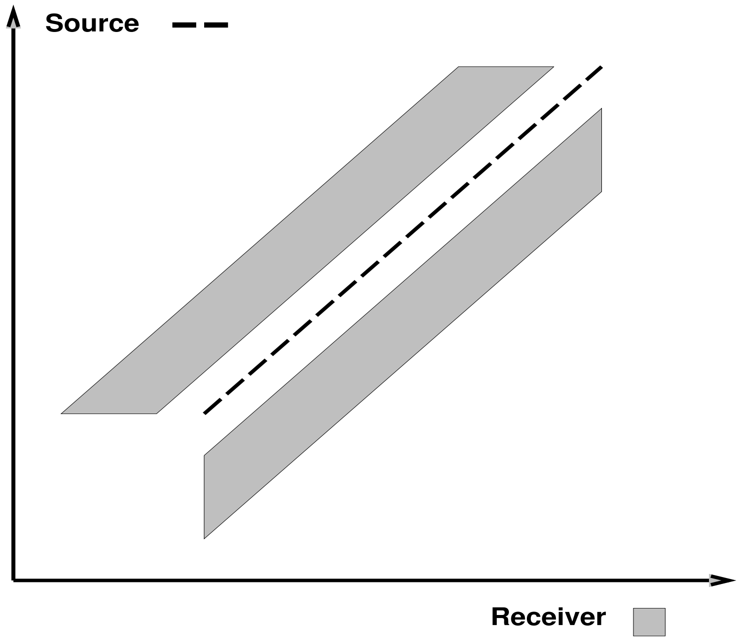

FIG. 3.3. The expanded acquisition pattern from the one-side spread using reciprocity. There are missing regions in the near and far offset. (interp-recp-acq) [NR]

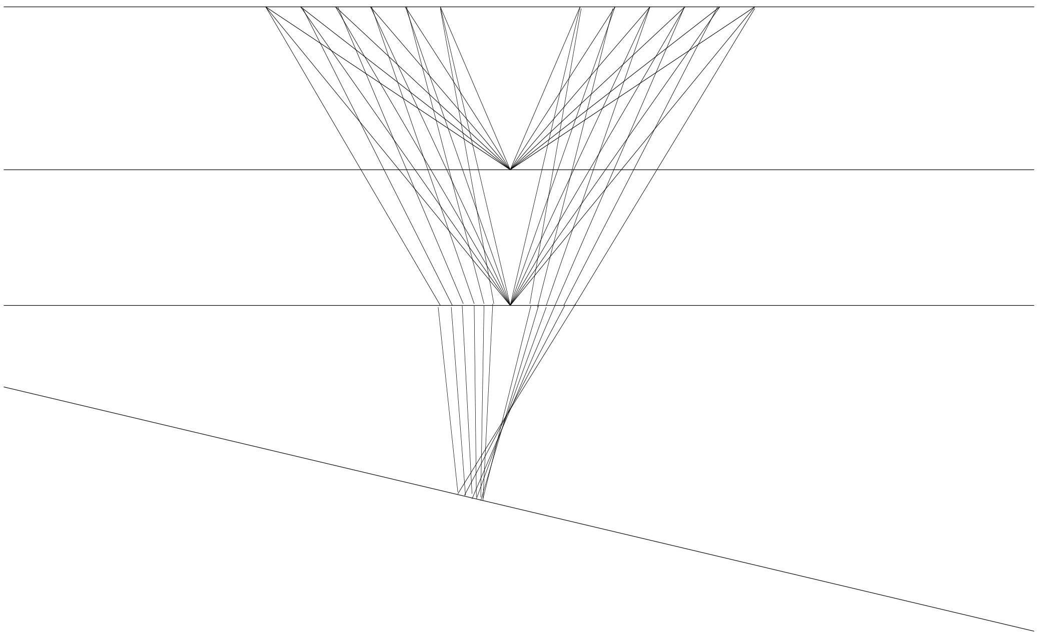

FIG. 3.4. Ray paths are depicted for a CMP gather. The effects of missing near-offset traces appear in different places according to the dips of reflectors. (interp-ang-cov) [NR]

3.3 Interpolation of missing near and far offsets

A method for restoring missing data is to regenerate from the model that fits to the known data. Since all reflection events are hyperbolic in CMP gathers, CMP gathers provide a good model for missing traces. Therefore, if we find the velocity spectrum that most closely produces the known data in a CMP gather, we can predict the missing data by hyperbolic modeling from the velocity spectrum.

Thus, the interpolation of missing near offset traces can be achieved in two steps. The first step is to find the best velocity spectrum from the known traces in each CMP gather. The search for the optimum velocity spectrum in the CMP gather can be formulated in a least-squares sense, as

$$0 \approx (\mathbf{d}_k - KH\mathbf{m})^2, \tag{3.2}$$

where $\mathbf{d}_k$ represents the known data in the CMP gather, $\mathbf{m}$ is the velocity spectrum, H is the hyperbolic modeling operator, and K is a diagonal matrix called a masking matrix (Claerbout, 1994) which has 1 where data is known and 0 where is missing as the element along the diagonal.

The second step is to model the missing traces from the optimum velocity spectrum, as follows:

$$\mathbf{d}_m = (I - K)H\mathbf{m}. \tag{3.3}$$

I have tested a simple synthetic CMP gather to verify the approach explained in the above. First, I put three spikes in a velocity spectrum and modeled a CMP gather by spreading the spectrum energy along the hyperbola, and then convolved the CMP gather with a Ricker wavelet (Figure 3.5). Figure 3.6 shows the interpolated CMP gather using the least-squares conjugate gradient algorithm. Because of the smoothness of the optimum velocity spectrum found by the least-squares method, the interpolated traces are close to the other traces in the near offset but not in the far offset.

In order to make the interpolated traces close to the other known traces, we need an optimum velocity spectrum which is spikier. To make the optimum velocity spectrum spiker, I used an adaptive weighting factor in the conjugate gradient. The velocity spectrum of the preceding step in each iteration is a good candidate for this problem, because the velocity spectrum has a larger value where we want to make the spiky spectrum than elsewhere after the first iteration. Thus, we solve the following iteratively-reweighted least-squares problem,

$$0 \approx (\mathbf{d}_k - KHW_i\mathbf{m}_i)^2 \tag{3.4}$$

with

$$W_i = |m_{i-1}|.$$

In equation (3.4), the subscript i represents the iteration step in the conjugate gradient. Figure 3.7 shows the interpolated CMP gather by using the adaptive weight least-squares method. Now we have an interpolated trace in the near and far offset that is closer to the known trace.

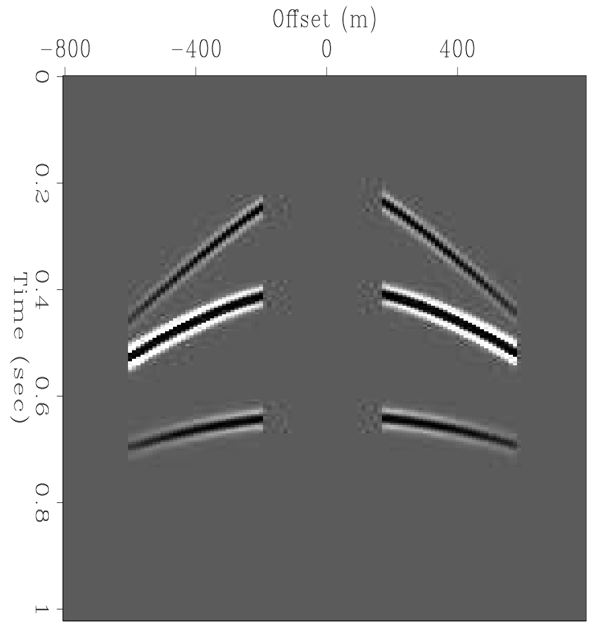

FIG. 3.5. Synthetic CMP gather with three reflectors with missing near and far offset traces. interp-syn-cmp [R]

3.4 Examples of the Marmousi data set

In order to see the effects of missing traces in a complex model, I tested the well-known Marmousi data set. Each shot gather of the Marmousi data set has the nearest offset traces at 175 meters from each shot location and leaves 8 near-offset traces missing. Figure 3.8 shows a CMP gather at 7500 meters along the surface location. The right half of the CMP gather is appended using the reciprocity principle. The interpolated gather appears

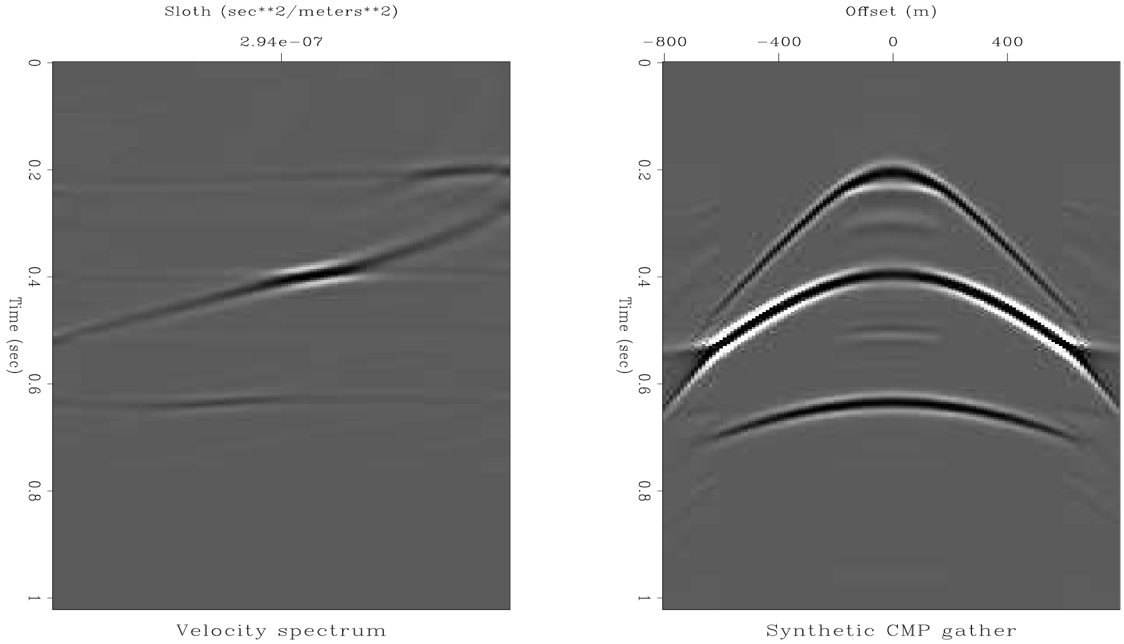

FIG. 3.6. Interpolated synthetic CMP gather without weighting in conjugate gradient iteration step. interp-syn-intcmp [CR]

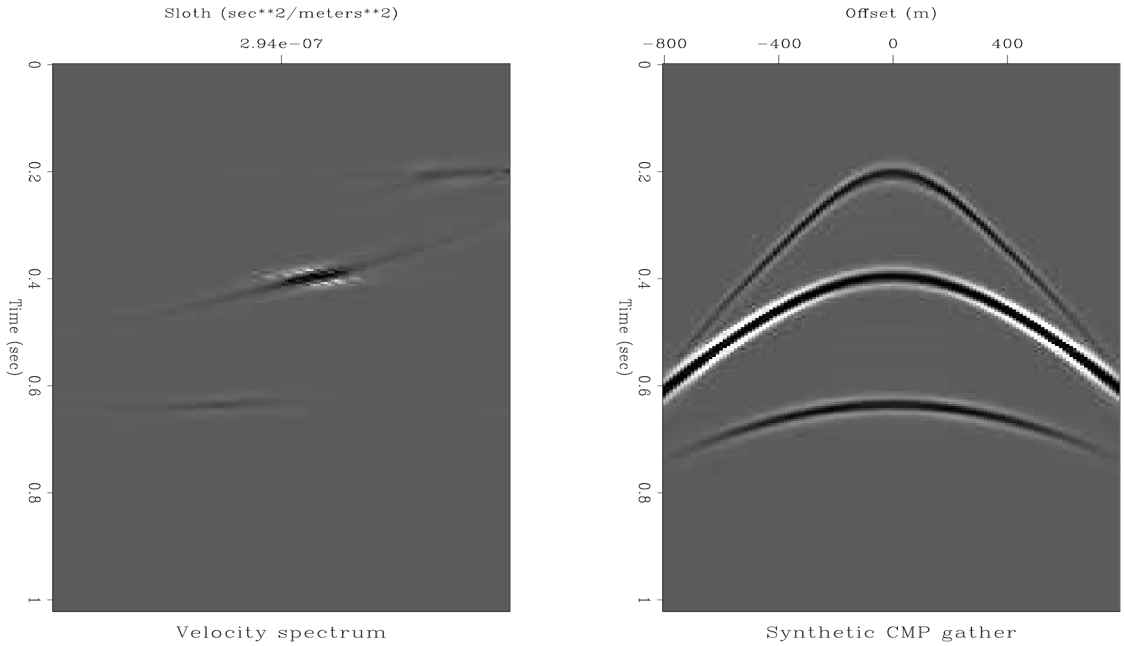

FIG. 3.7. Interpolated synthetic CMP gather with weighting in conjugate gradient iteration step. interp-syn-intcmpww [CR]

in Figure 3.9, which shows that the interpolated traces are very close to the known traces. Figures 3.10 and 3.11 show a common-shot gather at the shot location, 5100 meters, before and after interpolation of the whole CMP gathers, respectively; the interpolated traces follow the pattern of the other known reflection events very closely. Figures 3.12 and 3.13 show another example at a different shot location, 6250 meters, and demonstrate successful interpolation even for the weak events.

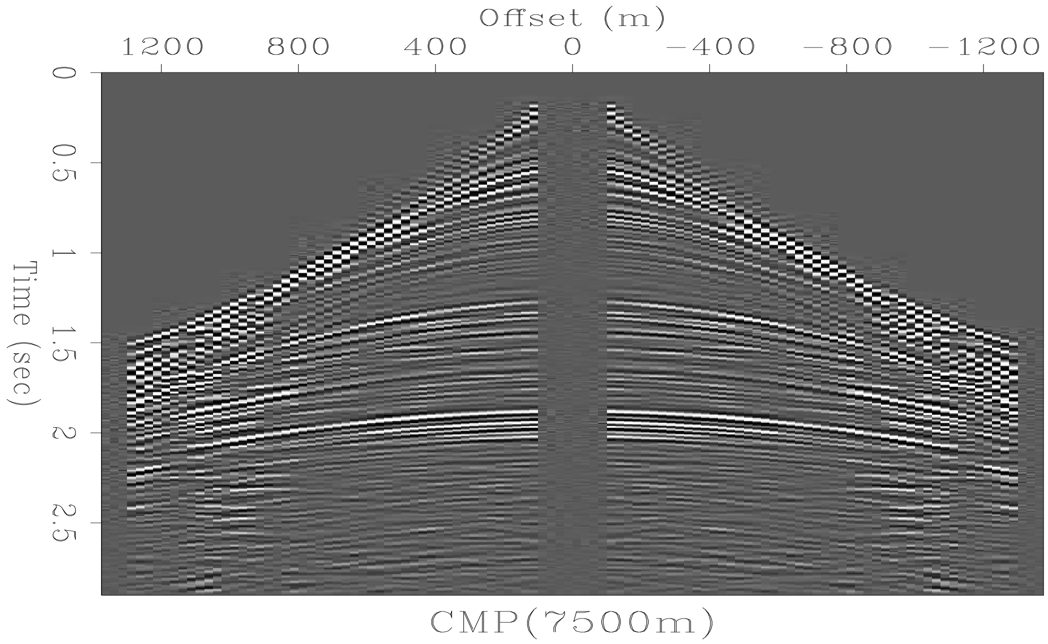

FIG. 3.8. CMP gather at 7500m in the Marmousi data set. interp-marm-cmp-463 [R]

In order to see the effects of missing traces in the plane-wave synthesis (PWS) imaging, I performed PWS imaging of the Marmousi data with missing near-offset traces and with interpolated near-offset traces. Figures 3.14 and 3.15 show the images of a zero-degree plane wave without and with near-offset traces, respectively. The major difference can be found around the flat reflector as annotated in the figure with question marks. Since the plane wave used in these examples travels vertically, most of reflected energy from flat reflectors would be in the near offset. Therefore, the missing near offset traces mostly affect the image of flat reflectors.

Figures 3.16 and 3.17 show the images of a 10-degree plane wave without and with near-offset traces, respectively. Again, the major difference appears around the reflector, which is close to 10-degrees, as annotated in the figure with question marks. This tells us

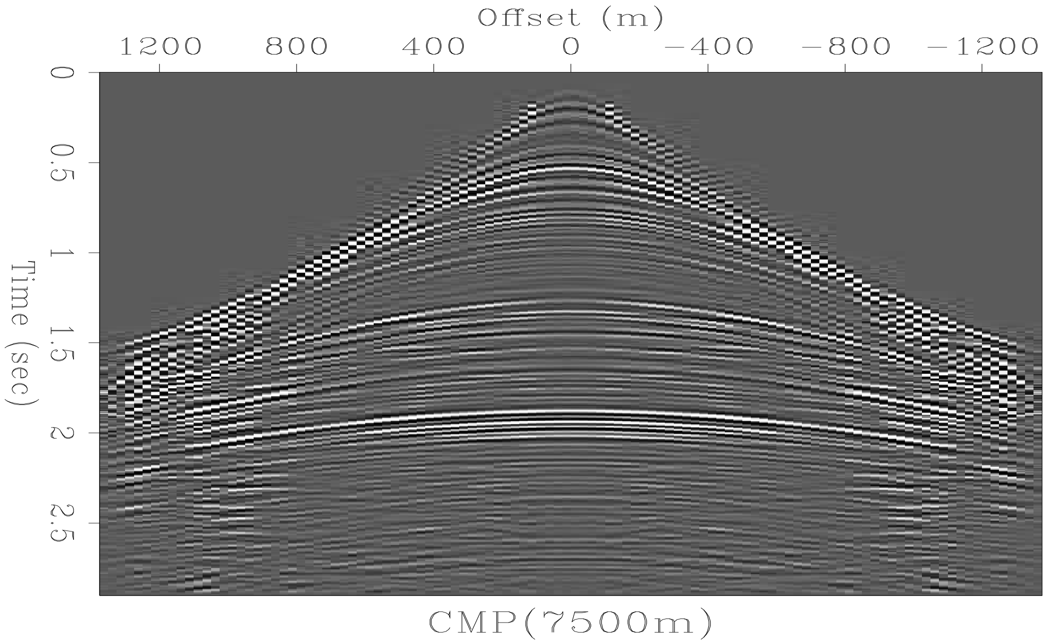

FIG. 3.9. Interpolated CMP gather at 7500m in the Marmousi data set. interp-marm-intcmp-463 [CR]

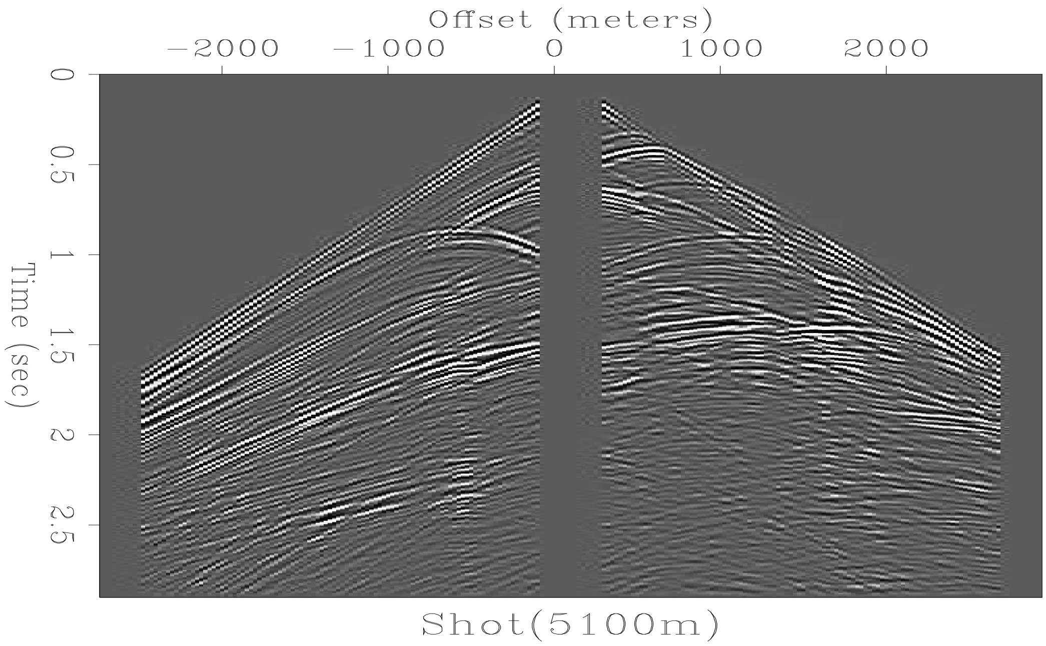

FIG. 3.10. Common shot gather at 5100m in the Marmousi data set. interp-marm-shot-85 [R]

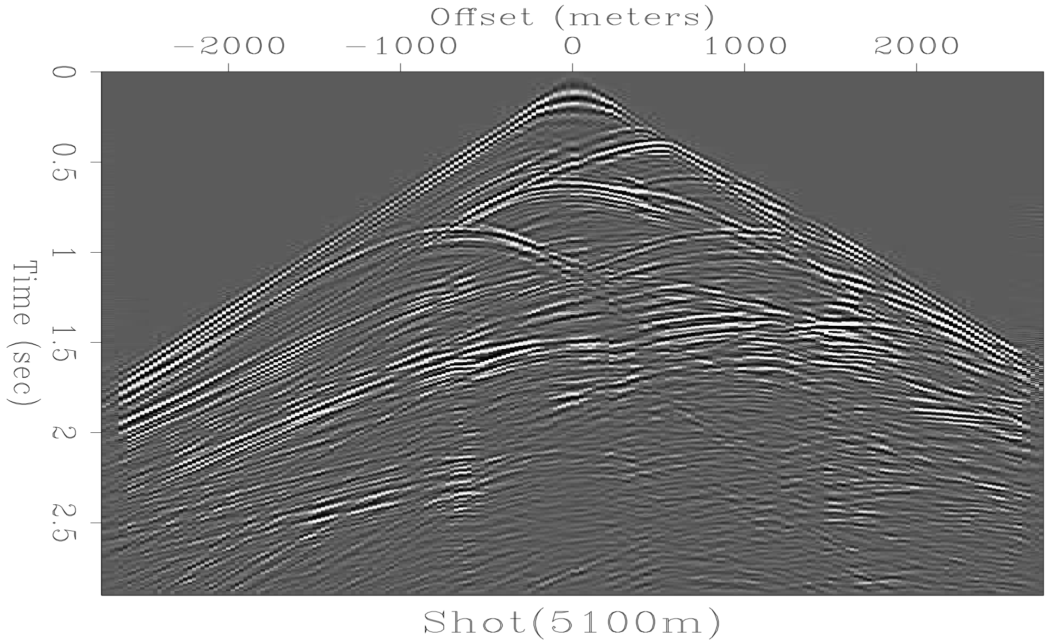

FIG. 3.11. Common shot gather at 5100m in the Marmousi data set after interpolation of the whole CMP gathers. interp-marm-intshot-85 [CR]

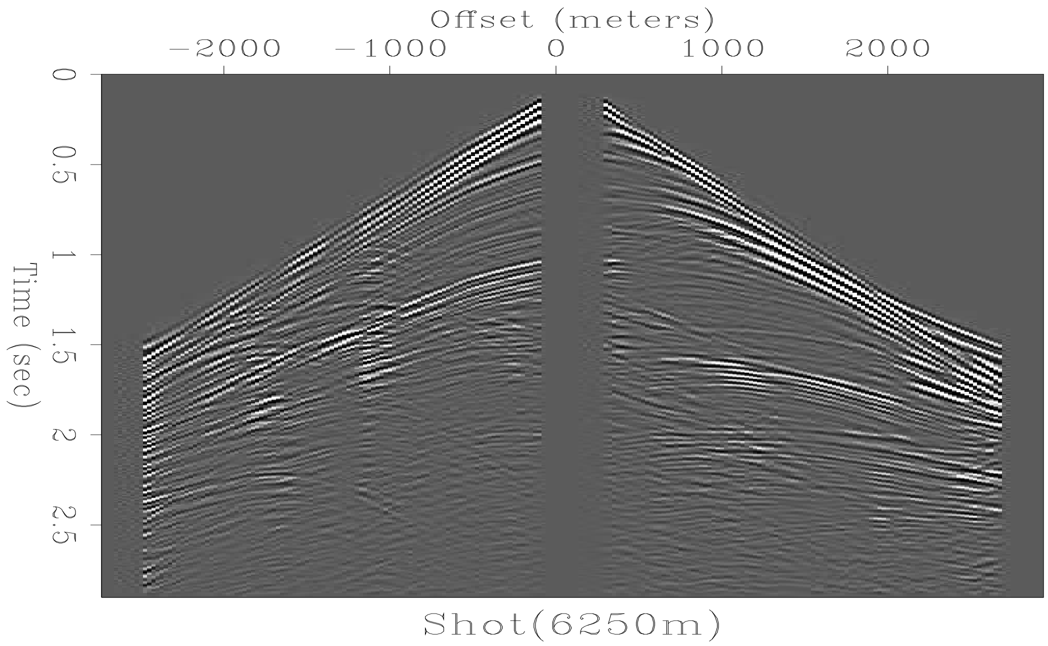

FIG. 3.12. Common shot gather at 6250m in the Marmousi data set. interp-marm-shot-131 [R]

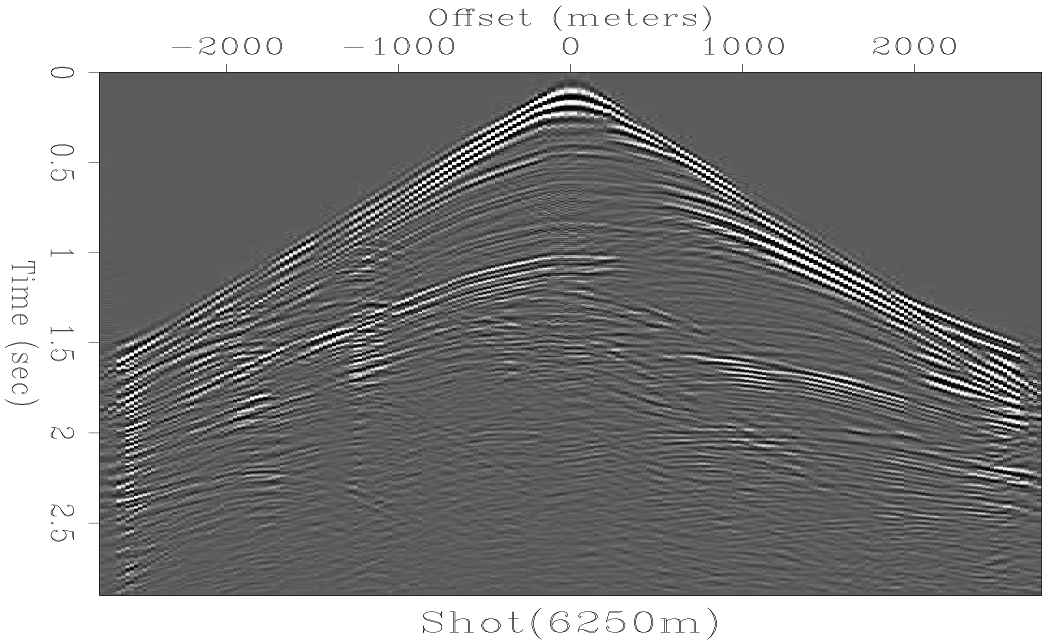

FIG. 3.13. Common shot gather at 6250m in the Marmousi data set after interpolation of the whole CMP gathers. interp-marm-intshot-131 [CR]

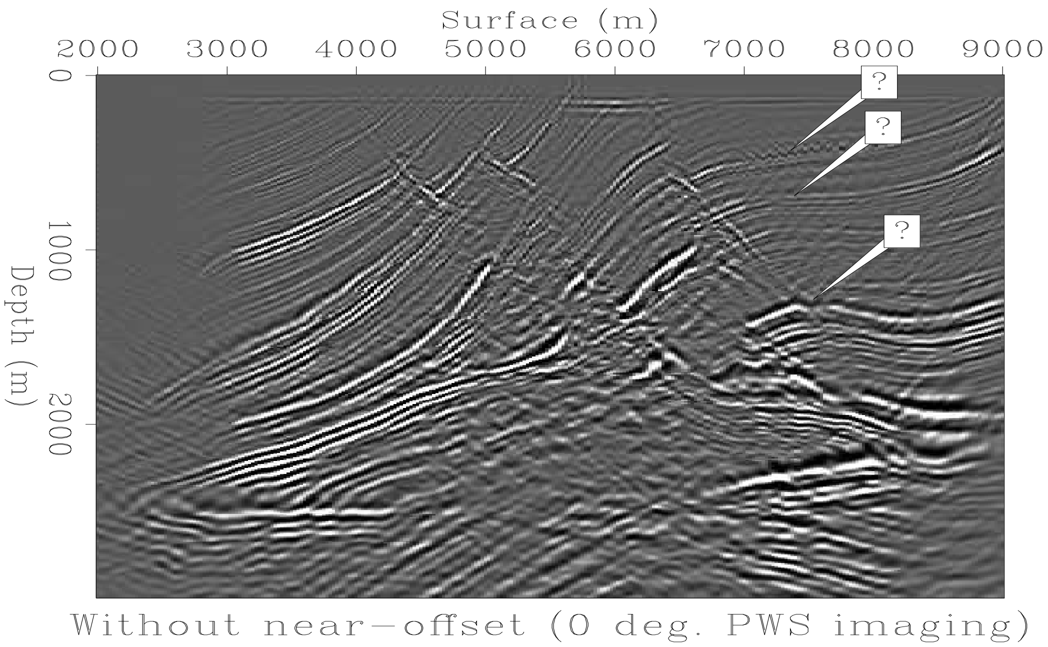

FIG. 3.14. Marmousi image without near offset traces, obtained by synthesizing a plane wave traveling vertically. interp-pws-mar-0 [CR]

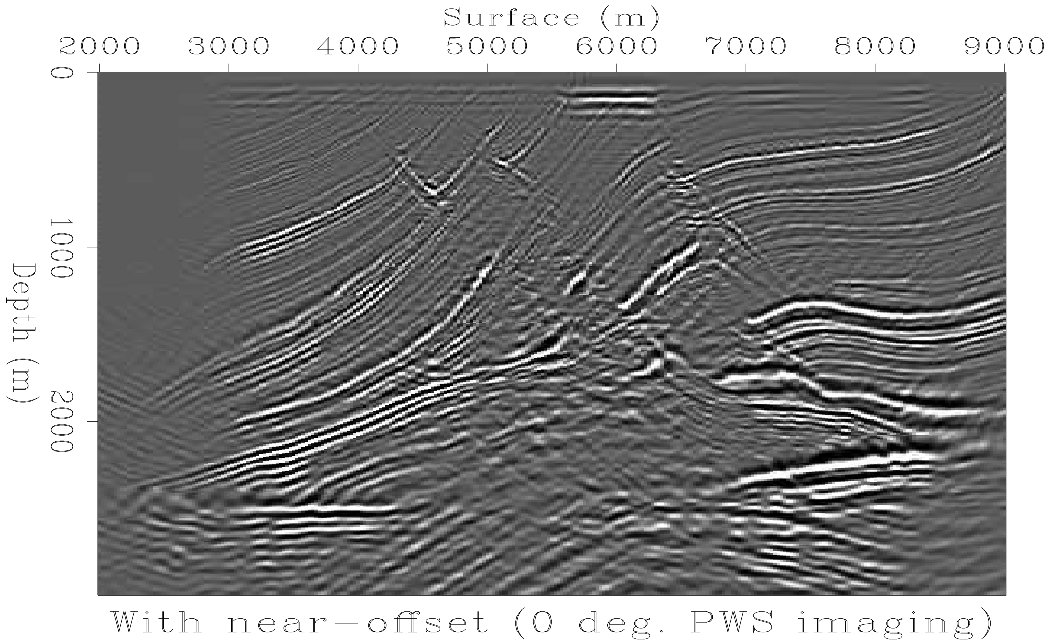

FIG. 3.15. Marmousi image with interpolated near offset traces, obtained by synthesizing a plane wave traveling vertically. interp-pws-marint-0 [CR]

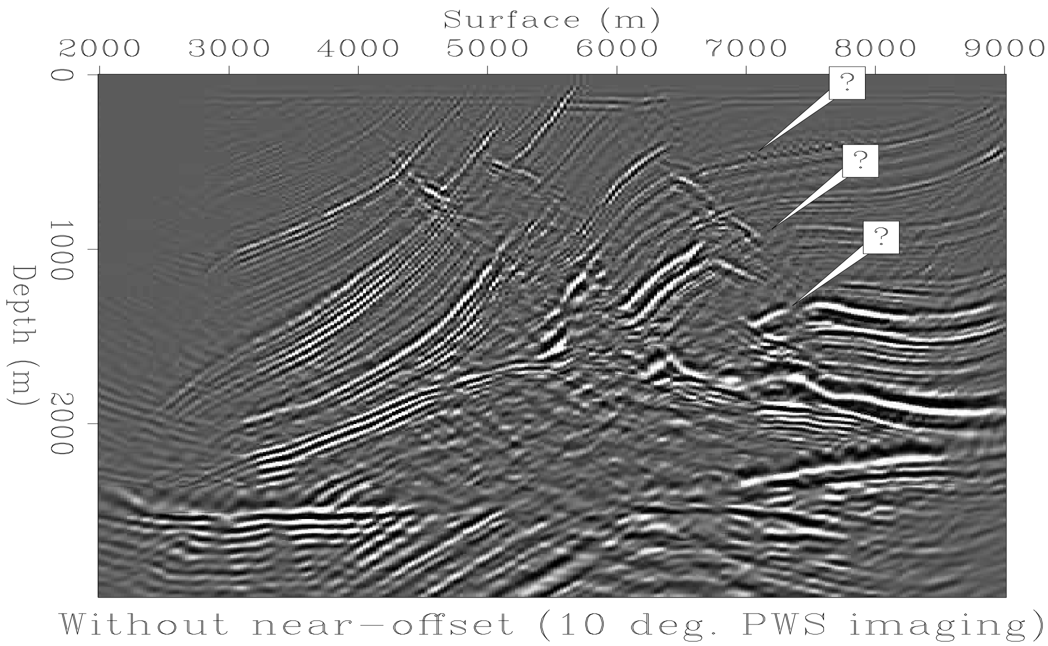

FIG. 3.16. Marmousi image without near offset traces, obtained by synthesizing a plane wave traveling 10 degrees to the vertical. interp-pws-mar-10 [CR]

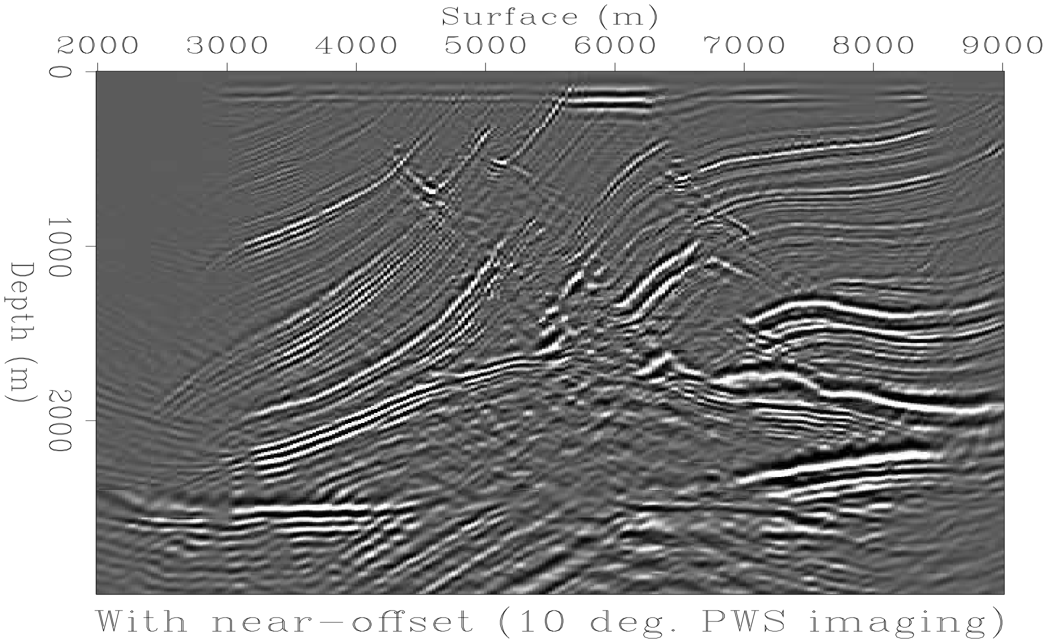

FIG. 3.17. Marmousi image with interpolated near offset traces, obtained by synthesizing a plane wave traveling 10 degrees to the vertical. interp-pws-marint-10 [CR]

that the missing near offset traces would affect the image quality of the reflectors whose dip is close to the dip of the synthesized plane wave.

3.5 Summary

Missing near-offset traces play an important role in wavefront synthesis imaging. The effect of missing near-offset appears as a weak or broken image from place to place according to the reflector geometry and the angle of the plane wave synthesized. I have developed an interpolation scheme to fill in the missing near-traces. After finding an optimum velocity spectrum of a common-midpoint (CMP) gather, the missing traces are filled in by hyperbolic modeling with the optimum velocity spectrum. In testing the method with the Marmousi data set, I recovered successfully the weak or broken images caused by missing traces by means of the interpolation algorithm.